

## NANOELECTRONIC DEVICE SIMULATION BASED ON THE WIGNER FUNCTION FORMALISM

HANS KOSINA

*Vienna University of Technology, Institute for Microelectronics  
Gusshausstrasse 27–29/E360, Vienna, A-1040, Austria  
kosina@iue.tuwien.ac.at*

Coherent transport in mesoscopic devices is well described by the Schrödinger equation supplemented by open boundary conditions. When electronic devices are operated at room temperature, however, a realistic transport model needs to include carrier scattering. In this work the kinetic equation for the Wigner function is employed as a model for dissipative quantum transport. Carrier scattering is treated in an approximate manner through a Boltzmann collision operator. A Monte Carlo technique for the solution of this kinetic equation has been developed, based on an interpretation of the Wigner potential operator as a generation term for numerical particles. Including a multi-valley semiconductor model and a self-consistent iteration scheme, the described Monte Carlo simulator can be used for routine device simulations. Applications to single barrier and double barrier structures are presented. The limitations of the numerical Wigner function approach are discussed.

*Keywords:* nanoelectronic devices, device simulation, Wigner function, kinetic equation, Monte Carlo method.

### 1. Introduction

For FETs with gate lengths below 10 nm quantum effects such as direct source-to-drain tunneling become important and start affecting the device characteristics<sup>1</sup>. Recent studies show that scattering will still affect the current<sup>2</sup> and that the transition to ballistic transport appears at much shorter gate lengths than previously anticipated<sup>3</sup>. An accurate theory of MOSFETs near the scaling limit must therefore account for the interplay between coherent quantum effects and dissipative scattering effects. This mixed transport regime can suitably be treated by the Wigner equation. Early numerical solutions of the Wigner equation were obtained using finite difference methods, assuming simplified scattering models based on the relaxation time approximation<sup>4</sup>. However, for realistic device simulation more comprehensive scattering models are required. With the advent of Monte Carlo (MC) methods for

the Wigner equation<sup>5,6</sup> it became feasible to include the full Boltzmann collision operator. The development of MC methods for the Wigner equation, however, is hampered by the fact that, as opposed to the semi-classical case, the integral kernel is no longer positive. This so-called negative sign problem will lead to exponentially growing variances of the Markov Chain MC method. The Wigner potential operator can also be viewed as a generation term of positive and negative numerical particles. In this picture the sign problem shows up in the avalanche of numerical particles generated. A stable MC method can only be achieved by means of a suitable particle annihilation algorithm.

## 2. The Physical Model

Quantum transport is modeled by a time-independent, one-electron Wigner equation for a multi-valley semiconductor. The set of Wigner equations is coupled through the inter-valley phonon scattering terms.

$$\begin{aligned} \frac{1}{\hbar} \left( \nabla_{\mathbf{k}} \epsilon_v(\mathbf{k}) \cdot \nabla_{\mathbf{r}} + \mathbf{F}(\mathbf{r}) \cdot \nabla_{\mathbf{k}} \right) f_v(\mathbf{k}, \mathbf{r}) = \\ \sum_{v'} \int [1 - f_v^0(\mathbf{k}, \mathbf{r})] S_{vv'}(\mathbf{k}, \mathbf{k}') f_{v'}(\mathbf{k}', \mathbf{r}) d^3 k' \\ - \left( \sum_{v'} \int [1 - f_{v'}^0(\mathbf{k}, \mathbf{r})] S_{v'v}(\mathbf{k}', \mathbf{k}) d^3 k' \right) f_v(\mathbf{k}, \mathbf{r}) \\ + \int V_w(\mathbf{k} - \mathbf{k}', \mathbf{r}) f_v(\mathbf{k}', \mathbf{r}) d^3 k' \end{aligned} \quad (1)$$

Silicon:  $v, v' = [100], [010], [001]$

This equation determines the Wigner function  $f_v$  for valley  $v$ . A valley's energy dispersion relation  $\epsilon_v(\mathbf{k})$  is assumed to be anisotropic and parabolic, resulting in a local diffusion term,  $\nabla_{\mathbf{k}} \epsilon_v \cdot \nabla_{\mathbf{r}} f$ . Note that a non-parabolic  $\epsilon(\mathbf{k})$  relation in the single-electron Hamiltonian would give a non-local diffusion term of the form  $\int \hat{\epsilon}(\mathbf{k}, \mathbf{r} - \mathbf{r}') f_v(\mathbf{k}, \mathbf{r}') d^3 r'$ .

A spectral decomposition of the potential profile  $V(\mathbf{r})$  is applied<sup>7</sup>. The slowly varying component gives the classical force  $\mathbf{F}$ , whereas the rapidly varying component is taken into account through the Wigner potential  $V_w$ .

$$V(\mathbf{r}) = V_{\text{cl}}(\mathbf{r}) + V_{\text{qm}}(\mathbf{r}) \quad (2)$$

$$\mathbf{F}(\mathbf{r}) = -\nabla V_{\text{cl}}(\mathbf{r}) \quad (3)$$

$$V_w(\mathbf{q}, \mathbf{r}) = \frac{1}{i\hbar} \int \left[ V_{\text{qm}}\left(\mathbf{r} + \frac{\mathbf{s}}{2}\right) - V_{\text{qm}}\left(\mathbf{r} - \frac{\mathbf{s}}{2}\right) \right] e^{-i\mathbf{q} \cdot \mathbf{r}} \frac{d^3 s}{(2\pi)^3} \quad (4)$$

In (1) scattering is treated semi-classically through a Boltzmann collision operator, where the transition rate  $S_{vv'}(\mathbf{k}, \mathbf{k}')$  from initial state  $(v', \mathbf{k}')$  to final state

$(v, \mathbf{k})$  is given by Fermi's golden rule. It should be noted that usage of the Boltzmann collision operator in the Wigner equation represents some ad hoc assumption. A rigorous treatment of electron-phonon scattering would require a frequency-dependent Wigner function,  $f(\mathbf{k}, \mathbf{r}, \omega)$ . It is related to the non-equilibrium Green's function  $G^<$  by  $G^<(\mathbf{r}, \mathbf{k}, \omega) = if(\mathbf{k}, \mathbf{r}, \omega)$  and can reasonably be approximated as<sup>8</sup>  $f(\mathbf{k}, \mathbf{r}, \omega) = f_w(\mathbf{k}, \mathbf{r})A(\mathbf{r}, \mathbf{k}, \omega)$ . To arrive at Fermi's golden rule the spectral function  $A$  is reduced to the Dirac  $\delta$ -function.

Furthermore, in (1) the Pauli blocking factor the equilibrium Fermi function  $f_v^0$  is used. The assumption of a Boltzmann collision operator in (1) ensures that in the semiclassical regions, such as the highly doped contact regions, the conductivity is finite and that the mean energy increase due to degeneracy is taken into account.

### 3. Numerical Methods

To solve (1) numerically, a stationary Monte Carlo method has been proposed, based on the interpretation of the potential operator  $\Theta[f_w] = \int V_w(\mathbf{k} - \mathbf{k}')f_w(\mathbf{k}', \mathbf{r})d^3k'$  as a generation term of numerical particles<sup>5</sup>. The mass conservation property of the potential operator can be exactly satisfied by the numerical particle model if one generates the numerical particles only pair-wise, for instance, with statistical weights  $+1$  and  $-1$ . A suitable annihilation algorithm for numerical particles needs to be introduced in order to achieve a stable Monte Carlo method. Since one can devise various algorithms for particle generation and, in particular, for particle annihilation, in the following the latest developments are described.

#### 3.1. Particle Generation

A direct numerical representation of the Wigner potential  $V_w(\mathbf{q}, \mathbf{r})$  would require the discretization of both momentum and space coordinates. The problem can be simplified by expressing the Wigner potential in terms of  $\hat{V}(\mathbf{q})$ , the Fourier transform of the potential  $V_{qm}(\mathbf{r})$ . The potential operator can be rewritten as follows.

$$\Theta_w[f_w](\mathbf{k}, \mathbf{r}) = \frac{1}{\hbar} \int |\hat{V}(\mathbf{q})| \sin[\varphi(\mathbf{q}) + \mathbf{q} \cdot \mathbf{r}] \times \left( f_w\left(\mathbf{k} - \frac{\mathbf{q}}{2}, \mathbf{r}, t\right) - f_w\left(\mathbf{k} + \frac{\mathbf{q}}{2}, \mathbf{r}, t\right) \right) \frac{d^3q}{(2\pi)^3} \quad (5)$$

An advantage of this formulation is that no discretization of the spatial variable  $\mathbf{r}$  is needed. The expression can be evaluated at the actual position  $\mathbf{r}$  of a particle. Only the momentum variable  $\mathbf{q}$  needs to be discretized in order to numerically represent  $|\hat{V}|$ , the modulus, and  $\varphi$ , the phase of  $\hat{V}$ .

The structure of (5) suggests the usage of a rejection technique. As a normalization quantity one obtains an upper limit for the pair generation rate.

$$\gamma_{\max} = \frac{1}{\hbar} \int |\hat{V}(\mathbf{q})| \frac{d^3q}{(2\pi)^3} \quad (6)$$

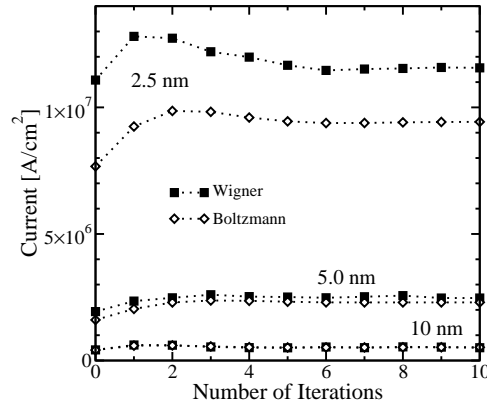


Fig. 1. Current through Si *n-i-n* diodes as a function of the number of self-consistent iterations with the width of the intrinsic region as a parameter.

At a rate of  $\gamma_{\max}$  the free flight of a particle is interrupted to check for particle pair-generation. From the distribution  $|\hat{V}(\mathbf{q})|$  one generates randomly the momentum transfer  $\mathbf{q}$ . Then the sine function is evaluated at the actual particle position  $\mathbf{r}$  as  $s = \sin[\varphi(\mathbf{q}) + \mathbf{q} \cdot \mathbf{r}]$ . With probability  $|s|$  the pair-generation event is accepted, otherwise a self-scattering event is performed. In the former case, two particle states are generated with momenta  $\mathbf{k}_1 = \mathbf{k} - \mathbf{q}/2$  and  $\mathbf{k}_2 = \mathbf{k} + \mathbf{q}/2$  and statistical weights  $w_1 = w_0 \text{sign}(s)$  and  $w_2 = -w_1$ , respectively, where  $w_0$  is the statistical weight of the initial particle. Since (5) is local in real space, the particle pair is generated at the position  $\mathbf{r}$  of the initial particle.

### 3.2. Particle Annihilation

Different variants of the single-particle Monte Carlo method can be devised<sup>5</sup>. The variant discussed in Ref.<sup>9</sup> guarantees exact current conservation. The only input parameter required is the ratio of negative and positive trajectories, which makes the algorithm easy to control. The idea is that from the trajectory tree generated by a particle injected at the contact only one branch is actually traced. For steady state problems considered here a phase space mesh can be utilized, on which numerical particles are temporarily stored. An annihilation mesh is introduced for each valley-type. The meshes are defined in the three-dimensional phase-space, spanned by one spatial and two momentum coordinates.

### 3.3. Coupling to the Poisson Equation

A self-consistent iteration scheme between Wigner MC and the Poisson equation is implemented. The adopted scheme, which is similar to the Gummel iteration scheme for the basic semiconductor equations<sup>10</sup>, is commonly used in classical one-particle

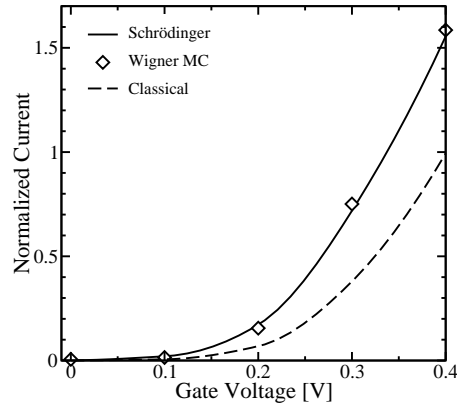


Fig. 2. Normalized ballistic currents calculated classically and quantum mechanically. Results from Wigner MC and the Schrödinger solver are in good agreement. The potential profile is obtained from a device simulation of a 10 nm gate length DG MOSFET.

MC simulations<sup>11</sup>. Fig. 1 shows the iteration history of the current through a Si *n-i-n* diode for different widths of the intrinsic region. Currents computed using Wigner and classical MC show similar convergence behavior.

#### 4. Results

The described MC method can be used for routine device simulations. For the purpose of verification, the first example assumes a frozen potential profile from a 10 nm gate length double-gate MOSFET. Fig. 2 compares the quantum ballistic currents as obtained from a collision-less Wigner MC simulation and from a numerical Schrödinger solver. Good agreement is observed. The quantum ballistic current is higher than the classical ballistic current due to an additional contribution from carriers tunneling through the potential barrier.

To study the effects of scattering and tunneling on the device characteristics we consider Si *n-i-n* diodes with the length  $W$  of the intrinsic region ranging from 20 nm down to 2.5 nm. The doping profile is assumed to increase gradually from the intrinsic region to the highly doped contact region over the same distance  $W$ . Three transport models are compared: Wigner equation and Boltzmann equation with electron-phonon and ionized-impurity scattering included, yielding currents  $I_{\text{WIG}}$  and  $I_{\text{BTE}}$ , respectively. The Wigner equation without scattering inside the intrinsic and transition regions gives the current  $I_{\text{COH}}$  (coherent). Fig. 3 shows that the effect of scattering reflected in the difference  $I_{\text{COH}} - I_{\text{WIG}}$  decreases with decreasing device length. However, even for  $W = 2.5$  nm the relative difference in the currents is still of the order of 25%, indicating that scattering cannot be neglected. Also shown is the current difference due to tunneling,  $I_{\text{WIG}} - I_{\text{BTE}}$ . Clearly, this current component rises with reduced barrier width.

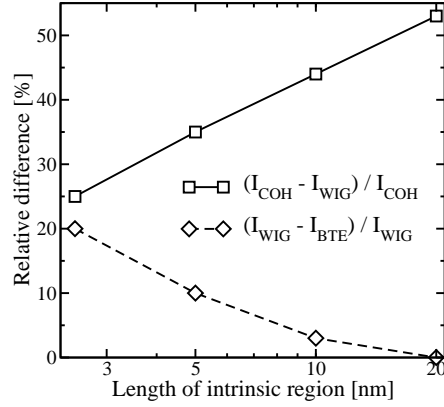


Fig. 3. Relative difference between currents of an  $n$ - $i$ - $n$  diode calculated using different transport models: Wigner MC with and without scattering in the intrinsic region (squares); Wigner MC and classical MC (diamonds).

## 5. Discussion

When using the Wigner equation for numerical simulation one should be aware of several peculiarities inherent to that approach. This approach is useful for a certain class of problems only, as briefly outlined below.

### 5.1. Interpretation of the Results

In many cases the quantities of interest are certain moments of the phase space distribution and not the full distribution itself. As in the classical case, the carrier density is given by the zeroth order moment and the current density by the first order moment. The second order moment is an energy like quantity. Its physical interpretation, however, is not obvious in the Wigner representation, but can be appreciated in the wave function representation.

In terms of the density operator  $\hat{\rho}(t)$  the carrier density is given by the diagonal element,  $n(\mathbf{r}, t) = \langle \mathbf{r} | \hat{\rho}(t) | \mathbf{r} \rangle$ , where  $|\mathbf{r}\rangle$  is the single-particle position eigenstate. With the momentum operator  $\hbar\hat{\mathbf{k}}$  the kinetic energy is related to the diagonal element of the operator  $\hat{\mathbf{k}}^2 \hat{\rho}$ . This operator needs to be symmetrized to guarantee real valued diagonal elements. For the symmetrized operator  $\hbar^2(\hat{\mathbf{k}}^2 \hat{\rho} + \hat{\rho} \hat{\mathbf{k}}^2)/(2m^*)$  the diagonal element evaluate to<sup>12</sup>

$$w(\mathbf{r}) = \sum_i p_i (E_i - V(\mathbf{r})) |\Psi_i(\mathbf{r})|^2 \quad (7)$$

where  $\psi_i$  denote the wave functions,  $E_i$  the eigen-energies, and  $p_i$  the probabilities determining the mixed state of the system.

The energy density (7) can become negative in tunneling regions where the energy of one or more states is below the band edge,  $E_i < V(\mathbf{r})$ . Transformation of

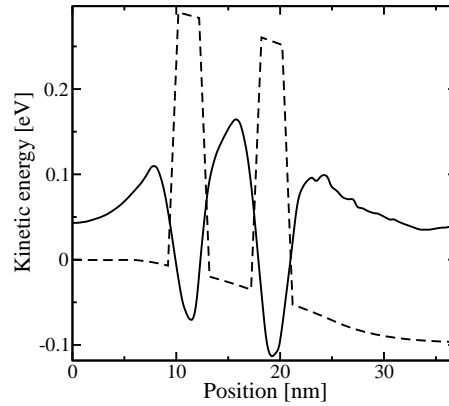


Fig. 4. Mean kinetic energy of electrons (solid line) in a resonant tunneling diode calculated from (8). In the tunneling barriers (dashed line) the mean kinetic energy is negative.

(7) into the Wigner representation gives<sup>12</sup>

$$w(\mathbf{r}) = \int \frac{\hbar^2}{2m^*} \left( |\mathbf{k}|^2 - \frac{1}{4} \nabla_{\mathbf{r}}^2 \right) f_w(\mathbf{k}, \mathbf{r}, t) \frac{d^3 k}{(2\pi)^3}. \quad (8)$$

Thus, the kinetic energy density is not simply given by the second moment of the Wigner function. A correction proportional to the second derivative of the electron concentration is required. Fig. 4 shows the kinetic energy density of electrons and the conduction band profile for a resonant tunneling diode.

### 5.2. The Bound-states Problem

For energy eigenstates,  $\psi_n(\mathbf{r}, t) = \psi_n(\mathbf{r}, 0) \exp(-\epsilon_n t/\hbar)$  the density matrix is time-independent,  $\rho_{nn}(\mathbf{r}_1, \mathbf{r}_2, t) = \psi_n^*(\mathbf{r}_1, 0) \psi_n(\mathbf{r}_2, 0)$ . In this case the system Hamiltonian and the density operator commute, and the quantum Liouville equation reduces to

$$i\hbar \frac{\partial \hat{\rho}}{\partial t} = [\hat{H}, \hat{\rho}] = 0. \quad (9)$$

This trivial equation, which does not contain the system Hamiltonian any longer, cannot determine bound-state density matrix. However, any given bound-state density matrix is time-independent and will satisfy this equation.

Since the quantum Liouville equation and the Wigner equation are linked by the Wigner-Weyl transform, similar arguments hold for the Wigner equation. It has been shown in Ref.<sup>13</sup> that bound states cannot be obtained from the following

Wigner equation for ballistic motion.

$$\left(\frac{\partial}{\partial t} + \frac{\hbar \mathbf{k}}{m^*} \cdot \nabla_{\mathbf{r}}\right) f_w(\mathbf{k}, \mathbf{r}, t) - \int V_w(\mathbf{k} - \mathbf{k}', \mathbf{r}) f_w(\mathbf{k}', \mathbf{r}, t) d^3 k' = 0 \quad (10)$$

$$V_w(\mathbf{q}, \mathbf{r}) = \frac{1}{i\hbar} \int \left\{ V\left(\mathbf{r} + \frac{\mathbf{s}}{2}\right) - V\left(\mathbf{r} - \frac{\mathbf{s}}{2}\right) \right\} e^{-i\mathbf{q} \cdot \mathbf{s}} \frac{d^3 s}{(2\pi)^3}$$

The harmonic oscillator is an example clearly demonstrating this problem. If the potential is a quadratic function of position,  $V(\mathbf{r}) = m^* \omega^2 |\mathbf{r}|^2 / 2$ , the Wigner equation (10) reduces to the corresponding classical Liouville equation, with  $\mathbf{F}(\mathbf{r}) = -m^* \omega^2 \mathbf{r}$  being the classical force.

$$\left(\frac{\partial}{\partial t} + \frac{\hbar \mathbf{k}}{m^*} \cdot \nabla_{\mathbf{r}} + \frac{\mathbf{F}(\mathbf{r})}{\hbar} \cdot \nabla_{\mathbf{k}}\right) f_w(\mathbf{k}, \mathbf{r}, t) = 0 \quad (11)$$

This equation propagates an initial distribution classically. Therefore, the single equation (10) is not completely equivalent to the Schrödinger equation. In the literature two independent solutions of this problem have been proposed.

Carruthers and Zachariasen<sup>13</sup> start from the Schrödinger equation and derive an adjoint Wigner equation. If this adjoint equation is considered in addition, the usual Schrödinger eigenvalue problem can be reconstructed from the two Wigner equations. The adjoint equation is obtained from a density matrix equation involving the anti-commutator<sup>13</sup>,  $[\hat{H}, \hat{\rho}]_+ = 2\epsilon \hat{\rho}$ , and takes the following form.

$$\frac{\hbar^2}{2m^*} \left( |\mathbf{k}|^2 - \frac{1}{4} \nabla_{\mathbf{r}}^2 \right) f_{mn}(\mathbf{k}, \mathbf{r}) - \int \tilde{V}_w(\mathbf{k} - \mathbf{k}', \mathbf{r}) f_{mn}(\mathbf{k}', \mathbf{r}) d^3 k'$$

$$= \frac{\epsilon_m + \epsilon_n}{2} f_{mn}(\mathbf{k}, \mathbf{r}) \quad (12)$$

$$\tilde{V}_w(\mathbf{q}, \mathbf{r}) = \frac{1}{2i\hbar} \int \left\{ V\left(\mathbf{r} + \frac{\mathbf{s}}{2}\right) + V\left(\mathbf{r} - \frac{\mathbf{s}}{2}\right) \right\} e^{-i\mathbf{q} \cdot \mathbf{s}} \frac{d^3 s}{(2\pi)^3}$$

The  $\epsilon_n$  are the eigenvalues of the Hamiltonian. For  $m = n$  one obtains the bound-state Wigner functions, which are real valued. The case  $m \neq n$  gives complex functions. The entire set of  $f_{mn}(\mathbf{k}, \mathbf{r})$  form a complete orthonormal set for all Wigner functions.

Tatarskii<sup>14</sup> takes as foundation the Wigner representation of quantum mechanics. The solutions of the Wigner equation have to be subjected to a necessary and sufficient condition which selects an allowed class of Wigner distributions describing quantum-mechanical pure states. The condition can be formulated in terms of the density matrix, obtained by the inverse Wigner-Weyl transform of the Wigner function, as follows<sup>14</sup>.

$$\nabla_{\mathbf{r}_1} \nabla_{\mathbf{r}_2} \ln \rho(\mathbf{r}_1, \mathbf{r}_2) = 0 \quad (13)$$

$$\rho(\mathbf{r}_1, \mathbf{r}_2) = \int f_w\left(\mathbf{k}, \frac{\mathbf{r}_1 + \mathbf{r}_2}{2}\right) e^{i\mathbf{k} \cdot (\mathbf{r}_1 - \mathbf{r}_2)} \frac{d^3 k}{(2\pi)^3} \quad (14)$$



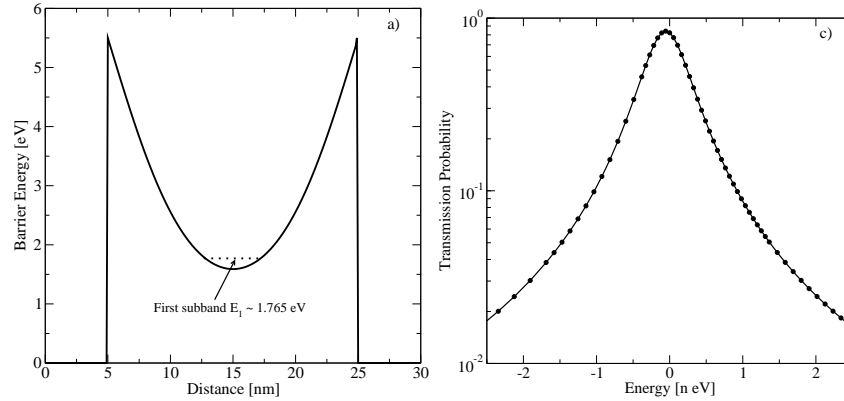


Fig. 5. Resonant tunneling structure with a quadratic potential well (a). The broadening of the first quasi-bound state is in the  $10^{-9}$ eV range (b).

As opposed to the adjoint equation (12), this condition is a pure mathematical one and does not contain any information about the system Hamiltonian. When condition (13) is satisfied, one can reconstruct the wave function up to a phase factor from the Wigner function. Furthermore, it can be shown that from the Wigner equation (10), with an initial condition satisfying the restriction (13) on the allowable form of pure state Wigner functions, the Schrödinger equation follows<sup>14</sup>. In the case of the harmonic oscillator, the quantization condition for the energy does not follow from the Wigner equation, but from the supplementary condition.

The fact that the Wigner equation alone cannot provide the bound-states of a closed system has some implications on the numerical solution methods, especially if the current through the system is determined by quasi-bound states of long life time. In this case the energy levels have very little broadening, which indicates that the system is almost closed. This situation is illustrated in Fig. 5 for the example of a resonant tunneling structure with a quadratic potential barrier. The spacing between resonance energies is constant for this potential. The first resonance peak of the transmission probability, calculated using a Schrödinger solver, is also shown in Fig. 5. To resolve this resonance a highly non-uniform energy grid with extremely small spacing around the resonance peaks is needed. The discrete Fourier transform utilized by a numerical Wigner equation solver, however, permits only equi-distant grids in momentum space. With such a grid the resonances for the above example cannot be resolved in practice, and the discrete Wigner equation would be ill-conditioned. From this discussion one can conclude that a numerical Wigner function approach is applicable only to sufficiently open systems, i.e., to systems with not too narrow resonances.

## 6. Conclusion

A Monte Carlo simulator performing a self-consistent numerical solution of the Wigner equation has been presented. Dissipation effects are included semi-classically through the Boltzmann collision operator. Algorithms for generation and annihilation of numerical particles have briefly been reviewed. The quantum Monte Carlo method turns gradually into the classical Monte Carlo method when the potential profile becomes smoother. Therefore, the simulation method can be used, for instance, to study the gradual emergence of quantum effects when a device structure is scaled down. While the numerical Wigner function approach can also handle the classical limit, it is unsuitable to describe closed quantum systems. The bound-state problem has been theoretically discussed in detail. It has been shown that the numerical Wigner function approach should only be applied to structures exhibiting not too narrow resonances.

## Acknowledgment

This work has been supported by the Austrian Science Fund, project I79-N16.

## References

1. J. Wang and M. Lundstrom, "Does Source-to-Drain Tunneling Limit the Ultimate Scaling of MOSFETs?," in *Int. Electron Devices Meeting*, pp. 29.2.1–29.2.4, IEEE, 2002.
2. P. Palestri, D. Esseni, S. Eminenti, C. Fiegna, E. Sangiorgi, and L. Selmi, "Understanding Quasi-Ballistic Transport in Nano-MOSFETs: Part I - Scattering in the Channel, and in the Drain," *IEEE Trans. Electron Devices*, vol. 52, no. 12, pp. 2727–2735, 2005.
3. M. Gilbert, R. Akis, and D. Ferry, "Phonon-Assisted Ballistic to Diffusive Crossover in Silicon Nanowire Transistors," *J. Appl. Phys.*, vol. 98, no. 9, pp. 094303–1–8, 2005.
4. W. Frensky, "Boundary Conditions for Open Quantum Systems Driven far from Equilibrium," *Rev. Mod. Phys.*, vol. 62, no. 3, pp. 745–789, 1990.
5. H. Kosina, M. Nedjalkov, and S. Selberherr, "A Monte Carlo Method Seamlessly Linking Classical and Quantum Transport Calculations," *Journal of Computational Electronics*, vol. 2, no. 2-4, pp. 147–151, 2003.
6. L. Shifren, C. Ringhofer, and D. Ferry, "Inclusion of Nonlocal Scattering in Quantum Transport," *Phys. Lett. A*, vol. 306, pp. 332–336, 2003.
7. A. Gehring and H. Kosina, "Wigner-Function Based Simulation of Classic and Ballistic Transport in Scaled DG-MOSFETs Using the Monte Carlo Method," *Journal of Computational Electronics*, vol. 4, pp. 67–70, 2005.
8. W. Hänsch, *The Drift-Diffusion Equation and Its Applications in MOSFET Modeling*. Computational Microelectronics, Wien New York: Springer Verlag, 1991.
9. H. Kosina, V. Sverdlov, and T. Grasser, "Wigner Monte Carlo Simulation: Particle Annihilation and Device Applications," in *Proc. Simulation of Semiconductor Processes and Devices*, (Monterey, CA, USA), pp. 357–360, Institute of Electrical and Electronics Engineers, Inc., Sept. 2006.
10. S. Selberherr, *Analysis and Simulation of Semiconductor Devices*. Wien: Springer, 1984.

11. F. Venturi, R. Smith, E. Sangiorgi, M. Pinto, and B. Ricco, "A General Purpose Device Simulator Coupling Poisson and Monte Carlo Transport with Applications to Deep Submicron MOSFET's," *IEEE Trans.Computer-Aided Design*, vol. 8, no. 4, pp. 360–369, 1989.
12. H. Kosina and M. Nedjalkov, *Handbook of Theoretical and Computational Nanotechnology*, vol. 10, ch. Wigner Function Based Device Modeling, pp. 731–763. Los Angeles: American Scientific Publishers, 2006. (in print).
13. P. Carruthers and F. Zachariasen, "Quantum Collision Theory with Phase-Space Distributions," *Rev.Mod.Phys.*, vol. 55, no. 1, pp. 245–285, 1983.
14. V. Tatarskii, "The Wigner Representation of Quantum Mechanics," *Sov.Phys.Usp.*, vol. 26, no. 4, pp. 311–327, 1983.